

## Helical Floquet Channels in 1D Lattices

Jan Carl Budich,<sup>1,2</sup> Ying Hu,<sup>1,3,4</sup> and Peter Zoller<sup>1</sup>

<sup>1</sup>*Institute for Quantum Optics and Quantum Information of the Austrian Academy of Sciences, 6020 Innsbruck, Austria and Institute for Theoretical Physics, University of Innsbruck, 6020 Innsbruck, Austria*

<sup>2</sup>*Department of Physics, University of Gothenburg, SE 412 96 Gothenburg, Sweden*

<sup>3</sup>*State Key Laboratory of Quantum Optics and Quantum Optics Devices, Institute of Laser Spectroscopy, Shanxi University, Taiyuan, Shanxi 030006, China*

<sup>4</sup>*Collaborative Innovation Center of Extreme Optics, Shanxi University, Taiyuan, Shanxi 030006, China*  
(Received 17 August 2016; published 7 March 2017)

We show how dispersionless channels exhibiting perfect spin-momentum locking can arise in a 1D lattice model. While such spectra are forbidden by fermion doubling in static 1D systems, here we demonstrate their appearance in the stroboscopic dynamics of a periodically driven system. Remarkably, this phenomenon does not rely on any adiabatic assumptions, in contrast to the well known Thouless pump and related models of adiabatic spin pumps. The proposed setup is shown to be experimentally feasible with state-of-the-art techniques used to control ultracold alkaline earth atoms in optical lattices.

DOI: 10.1103/PhysRevLett.118.105302

**Introduction.**—Exploring the rich phenomenology of spin-orbit coupling is an active field of research in numerous branches of quantum physics [1–3]. The discovery of helical edge states [4–6] has opened the route towards perfect spin-momentum locking, characterized by a one-to-one correspondence between the propagation direction of particles and their spin. Such exotic states have only been realized at the surface of 2D topological insulators [4,7–10]. Without the 2D bulk, their occurrence is forbidden in 1D lattice systems [10], as the periodicity of band structures in the first Brillouin zone (BZ) imposes fundamental constraints—referred to as fermion doubling [11] [cf. Fig. 1(a)]. Harnessing the unique properties of periodically driven quantum systems [12–17], here we show how these limitations can be circumvented: we find perfect spin-momentum locking in the stroboscopic dynamics of a periodically driven 1D lattice model. While conventional helical edge states require a time-reversal symmetric topological 2D bulk [18], the spin-momentum locking in our 1D setting stems from topological properties in combined time-momentum (Floquet) space [see Fig. 1(d)], and relies on a spin-rotation symmetry of the stroboscopic dynamics. Our approach goes conceptually beyond adiabatically projected models such as the Thouless pump [19,20], in that we consider the full quasienergy spectrum without involving adiabatic projections.

In Floquet systems, the quasienergies are only defined modulo the driving frequency  $\Omega$ , allowing for spectra that are only periodic in the BZ up to integer multiples of  $\Omega$ . However, even in driven systems, unidirectional motion in 1D systems cannot be achieved without adiabatic assumptions, due to fundamental topological constraints [21]. The central result of this Letter is that the Floquet Bloch Hamiltonian ( $\hbar = 1$ )

$$H^F = vk\sigma_z \quad (1)$$

exhibiting the perfect spin-momentum locking [see Fig. 1(c)] familiar from the helical edge states of 2D topological insulators can still be achieved in a microscopic

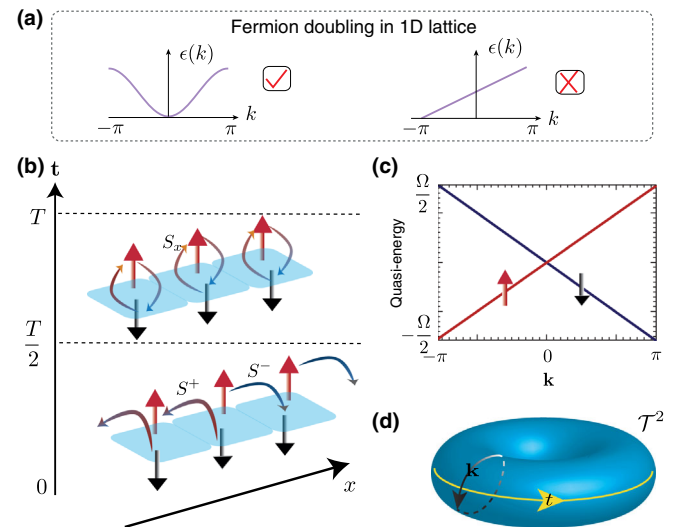


FIG. 1. (a) Illustration of basic constraints by fermion doubling in 1D lattice systems: The left plot shows an ordinary metallic band which must be periodic in the first Brillouin zone, while the unidirectional channel in the right plot violates this periodicity and, hence, is forbidden by fermion doubling. (b) Schematic of the proposed driving protocol. The spin-flip hopping [see  $H_1$  in Eq. (2)] acts during the first half-period  $[0, T/2)$ , while on-site spin flips [see  $H_2$  in Eq. (2)] characterize the second half-period  $[T/2, T)$ . (c) Floquet band structure of the proposed lattice model [see Eqs. (2), (3)] with perfect spin-momentum locking. Parameters are  $\alpha = \beta = \pi/T$ . (d) Illustration of the toroidal time-momentum space  $T^2$ .

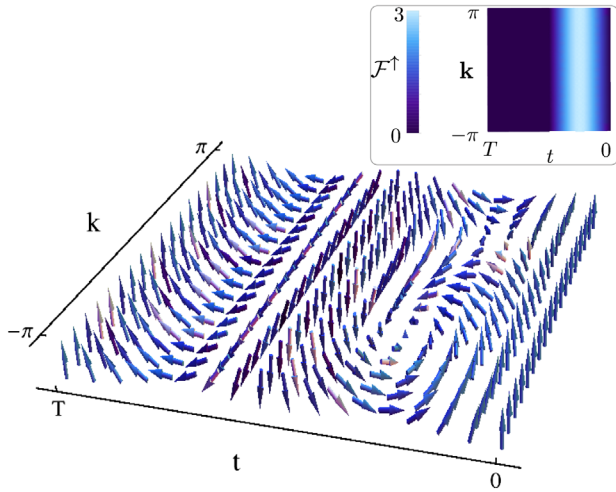


FIG. 2. Lower panel: Topologically nontrivial spin micromotion of the Bloch states  $|u_k^\uparrow(t)\rangle = U_k(t,0)|u_k^\uparrow(0)\rangle$  that are eigenstates of the spin-up Floquet operator  $U_k^\uparrow(T,0)$  at stroboscopic times  $t = 0 \pmod{T}$ . Upper panel: Berry curvature  $\mathcal{F}_{k,t}^\uparrow = 2\text{Im}\{\langle \partial_k u_k^\uparrow(t) | \partial_t u_k^\uparrow(t) \rangle\}$  in combined time-momentum space. Parameters are  $\alpha = \beta = \pi/T = \pi$  in all plots.

1D lattice model. Equation (1), with the lattice momentum  $k$  and standard Pauli matrix  $\sigma_z$ , describes two spin species that independently perform an opposite unidirectional and dispersionless motion with velocity  $v$ .

Remarkably, such behavior is possible beyond adiabatic dynamics even though the unidirectional motion of a single spin species cannot be achieved. To see this, we note that  $H^F$  in a Floquet system generates the stroboscopic dynamics described by the time-evolution operator  $U(T,0) = e^{-iH^F T}$  over one driving period  $[0, T)$  with  $T = 2\pi/\Omega$ . During the so-called micromotion within a period, the two spin species are necessarily intertwined in a topologically nontrivial fashion [see Fig. 1(b) and Fig. 2] as we discuss below. In addition, we provide an experimentally feasible proposal for realizing this scenario with ultracold alkaline earth atoms (AEAs) in optical lattices.

*Lattice model with perfect spin-momentum locking.*—We consider a Floquet system of fermions with spin  $1/2$  annihilated by the spinor operators  $\psi_j = (\psi_{j\uparrow}, \psi_{j\downarrow})$  on a 1D lattice with unit lattice constant. The driving protocol consists of switching between two noncommuting time-independent Hamiltonians  $H_1$  and  $H_2$ , such that  $H_1$  generates the time evolution during the first half-period  $[0, T/2) \pmod{T}$  whereas  $H_2$  operates during the second half-period  $[T/2, T) \pmod{T}$ . The explicit form of  $H_1$  and  $H_2$  reads as [see Fig. 1(b) for an illustration]

$$H_1 = -\alpha \sum_j \psi_j^\dagger S^+ \psi_{j+1} + \text{H.c.}, \quad H_2 = \beta \sum_j \psi_j^\dagger \sigma_x \psi_j, \quad (2)$$

where  $S^+ = \frac{1}{2}(\sigma_x + i\sigma_y)$  flips the spin from down to up and  $\alpha, \beta$  are real coupling constants [22]. Both  $H_1$  and  $H_2$  are lattice translation invariant, rendering the lattice momentum  $k$  a good quantum number and allowing us to factorize the time-evolution operator into momentum components  $U_k(t, t_0)$ . For the parameter choice  $\alpha = \beta = \pi/T$ , we obtain

$$U_k(T, 0) = e^{-iH_2^k T/2} e^{-iH_1^k T/2} = e^{-ik\sigma_z}, \quad (3)$$

where  $H_1^k = -\alpha[\cos(k)\sigma_x - \sin(k)\sigma_y]$  and  $H_2^k = \beta\sigma_x$  are the Bloch Hamiltonians associated with  $H_1$  and  $H_2$  [see Eq. (2)], respectively. Computing the associated Floquet Bloch Hamiltonian  $H_k^F = (i/T) \log[U_k(T, 0)] = (1/T)k\sigma_z$ , we recover Eq. (1) with the velocity  $v = 1/T$ . Note that  $H_k^F$ , when interpreted as a static Bloch Hamiltonian, contains a discontinuous jump at  $k = \pm\pi$  and, hence, cannot be achieved by any (local) hopping in real space. Quite remarkably, in the present Floquet setting, it can be achieved—or practically at least be arbitrarily closely approached—by simply tuning the parameters  $\alpha$  and  $\beta$  in the local instantaneous Hamiltonians (2).

The spin-momentum locking in the proposed Floquet system may be understood at an intuitive level [see also Fig. 1(b)]. The Hamiltonian  $H_1$  drives a hopping process between nearest-neighbor sites during the first half-period, where opposite directions of motion are tied to opposite spin-flip operations. However, once a particle has hopped, it has the wrong spin to hop into the same direction again, since  $(S^+)^2 = 0$ . To prevent this deadlock,  $H_2$  recharges the spin-pump during the second half-period by flipping back the spin on site. Putting together the two half-cycles, each particle has moved by one site with a perfect spin-momentum locking after a full period.

*Implementation with alkaline earth atoms.*—The lattice model [(2), (3)] may be experimentally implemented with state-of-the-art techniques for the control of ultracold atoms [see Ref. [23] for a review], where Raman processes are employed to design laser-assisted hopping in optical lattices [24–28]. An ideal experimental platform in this context is provided by gases of AEAs such as Yb [see, e.g., Ref. [27]]. There, the spin degree of freedom  $\sigma$  occurring in our model is encoded in two Zeeman levels with different magnetic quantum number  $m_F$  of the atomic ground state of  $^{173}\text{Yb}$ . Spin-flip processes are then controlled by optical dipole selection rules of the involved Raman transitions. A detailed proposal for the implementation of the spin-flip hopping characterizing  $H_1$  based on the experimental tools of Ref. [27] has recently been published [29]. The on-site spin-flip processes defining  $H_2$  have already been extensively employed experimentally [27] to realize hopping in so-called synthetic dimensions [30,31], where internal states of the atom are interpreted as lattice sites in an extra dimension. To experimentally realize our two-step driving protocol [see Fig. 1(b)], we propose to use pulsed Raman

lasers switching between laser-assisted spin-flip hopping ( $H_1$ ) and on-site spin flips ( $H_2$ ). An alternative implementation of our model may be provided by a superlattice setting with double-well supersites encoding the spin degrees of freedom, which can be readily implemented using alkali atoms [20].

*Topological analysis.*—We now provide a deeper understanding in terms of topology of how the phenomenology discussed above can arise in a microscopic lattice model without relying on adiabatic projections. We stress the different role of topology in our present setting, as compared to conventional helical edge states. In 2D topological insulators, a topological invariant associated with the time-reversal invariant insulating bulk of the system entails and protects the presence of helical edge states [4,10]. Here, instead, an emergent spin-rotation symmetry in the stroboscopic dynamics of the 1D system allows for the definition of a topological invariant that entails and protects helical Floquet modes as described by Eq. (1). The protecting symmetry of the Floquet spectrum (Floquet symmetry) in our model (2) requires tuning the system to the parameter line  $\alpha = \beta = \pi/T$ . However, below we show with numerical simulations [see Fig. 3] that, even in the presence of significant deviations from this ideal situation, clear signatures of the spin-momentum locking are still experimentally observable. The Floquet operator  $U_k(T, 0)$  in Eq. (3) with  $\alpha = \beta = \pi/T$  preserves  $S_z = \sigma_z/2$  and can, hence, be decomposed into two irreducible blocks  $U_k^\sigma(T, 0)$ ,  $\sigma = \uparrow, \downarrow$ . The Floquet winding number [21] for the individual spin blocks reads as

$$\nu_\sigma = \frac{1}{2\pi i} \oint_{\text{BZ}} dk \text{Tr}[U_k^\sigma \partial_k U_k^{\sigma\dagger}] = \frac{1}{\Omega} \oint_{\text{BZ}} dk \sum_\alpha (\partial_k \epsilon_k^{\sigma, \alpha}) \quad (4)$$

with the Floquet quasienergies  $\epsilon_k^{\sigma, \alpha}$  for band  $\alpha$  in spin block  $\sigma$ . We note that in our specific model, there is only one band per spin block. The topological invariant  $\nu_\sigma$  simply counts the number of chiral Floquet modes with spin  $\sigma$ , i.e., Floquet bands which are periodic in the BZ only modulo  $\Omega$ . For the model in Eq. (3),  $\nu_\sigma = \pm 1$  for  $\sigma = \uparrow, \downarrow$ .

In Ref. [21], a similar Floquet winding number  $\nu$  has been introduced, counting the total number of chiral Floquet modes without assuming a spin-rotation symmetry. Furthermore, it has been shown that  $\nu$  is identical to the Chern number [32,33] of the 2D system characterized by the Bloch functions  $|u_k^\alpha(t)\rangle = U_k(t, 0)|u_k^\alpha(0)\rangle$  in combined  $(k, t)$  space [see Fig. 1(d)], where  $\alpha$  labels the Floquet Bloch bands and  $|u_k^\alpha(0)\rangle$  is family of eigenfunctions of the Floquet operator  $U_k(T, 0)$ . This relation implies that a nonzero  $\nu$  can only occur in effective models such as the Thouless pump [19], where some energetically higher-lying bands have been adiabatically eliminated before computing the Floquet quasiband structure. This is because the Chern numbers of all bands obey a zero-sum rule in lattice models. The intuitive picture behind this rule is that

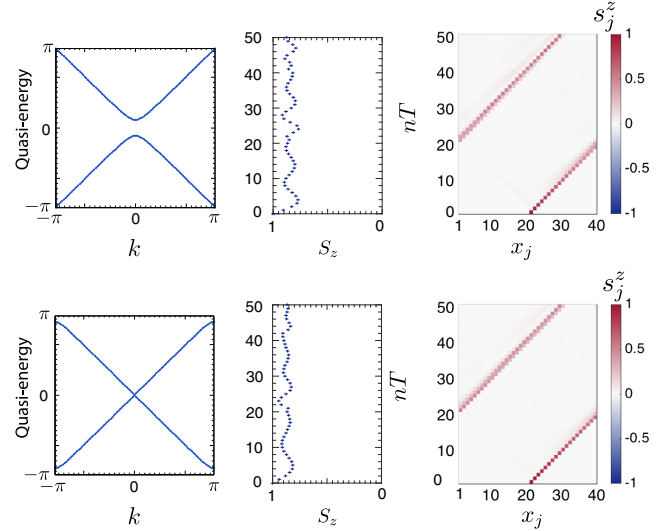


FIG. 3. Top: Gap around  $k = 0$  for  $\alpha = 1.1\pi/T$ ,  $\beta = 0.9\pi/T$ . From left to right, the three plots show the Floquet spectrum of the system, the total  $S_z$  polarization as a function of time, and the spatially resolved  $S_z$  polarization as a function of time. Bottom: Gap around  $k = \pi$  for  $\alpha = \beta = 0.92\pi/T$ . The plots are analogous to those in the top panel.

the Chern number of a subspace with projection  $P(k, t) = \sum_\alpha |u_k^\alpha(t)\rangle \langle u_k^\alpha(t)|$  measures the winding of the orientation of this subspace in the total Hilbert space. If the considered Floquet system contains all bands, we have  $P(k, t) = \mathbf{1}$  and no nontrivial winding is possible.

By contrast, in our microscopic lattice model [(2), (3)], a nontrivial  $\nu_\sigma$  is possible because the two spin species are intertwined during the micromotion, i.e., by the time-evolution operator  $U_k(t, 0)$ ,  $0 < t < T$ . The resulting winding in spin space of the Bloch functions  $|u_k^\uparrow(t)\rangle = U_k(t, 0)|u_k^\uparrow(0)\rangle$  with  $|u_k^\uparrow(0)\rangle$  denoting an eigenfunction of  $U_k^\uparrow(T, 0)$  is shown in the lower panel of Fig. 2. The Berry curvature  $\mathcal{F}_{k,t}^\uparrow = 2\text{Im}\{\langle \partial_k u_k^\uparrow(t) | \partial_t u_k^\uparrow(t) \rangle\}$  is shown in the upper panel of Fig. 2. Computing the Chern number  $\mathcal{C}^\uparrow$  associated with the toroidal combined momentum-time space  $\mathcal{T}^2$  [see Fig. 1(d)] yields  $\mathcal{C}^\uparrow = (1/2\pi) \int_{\mathcal{T}^2} \mathcal{F}^\uparrow = \nu_\uparrow = 1$ , and, in agreement with the mentioned zero-sum rule of Chern numbers,  $\mathcal{C}^\downarrow = \nu_\downarrow = -1$ .

*Stability of spin-momentum locking.*—We now show that the spin-momentum locking stays robust and clearly observable even in the presence of deviations from the parameter line  $\alpha = \beta = \pi/T$  representing possible experimental imperfections.

We first study the visibility of the spin-momentum locking for a localized wave packet initialized at site  $j = 21$  with spin-up polarization. We numerically simulate a system with a size of  $L = 40$  lattice sites. In the following, we focus on periodic boundary conditions, noting that open boundary conditions simply lead to a perfect reflection of the particles involving a spin flip on the

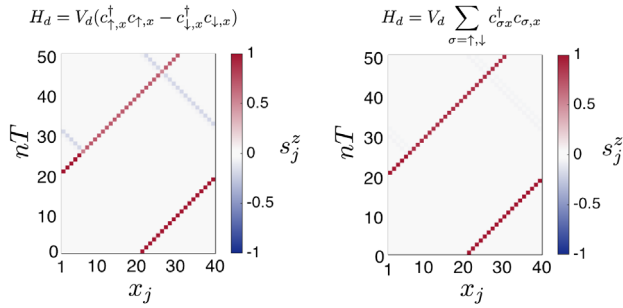


FIG. 4. Left: Scattering due to  $\sigma_z$  impurity at site  $x = 6$ . The plot shows the spatial distribution of the  $S_z$  polarization as a function of time. Right: Scattering due to  $\sigma_0$  impurity at site  $x = 6$ . The bulk parameters are  $\alpha = \beta = \pi/T$  and  $V_d = 1.5/T$  in both plots.

outermost sites. In Fig. 3, we summarize our results if (i) a gap around  $k = 0$  is opened in the quasienergy spectrum by setting  $\alpha \neq \beta$  (see top panel), and (ii) if a gap is opened around  $k = \pm\pi$  for  $\alpha = \beta \neq \pi/T$  (see bottom panel). The effects of such imperfections are twofold. First, due to the deviation from a perfectly linear dispersion, the initially sharply localized wave packet slightly spreads out in real space. Second, due to a coupling of the two spins, a finite spectral weight of the opposite spin species ( $< 5\%$  for a relative deviation of  $10\%$  in the system parameters) is generated. Our numerical data show that the spin-momentum locking is still clearly visible, even for significant deviations from the ideal parameter line  $\alpha = \beta = \pi/T$ .

Generally speaking, in the presence of symmetry breaking imperfections, a gap may open around  $\Omega/2$  in the quasienergy spectrum. However, when interpreting the resulting  $H_k^F$  as a static band structure, it would still be extremely challenging to realize, as the corresponding decay length of the hopping range in real space diverges on approaching the parameter line  $\alpha = \beta = \pi/T$ . Instead, in the present Floquet scheme, an arbitrarily nonlocal  $H_k^F$  exhibiting arbitrarily precise spin-momentum locking can readily be experimentally achieved by (approximately) tuning the local coupling strengths  $\alpha$  and  $\beta$ .

In addition, we study the influence of various imperfections that break the translation invariance in our system (see Fig. 4). Specifically, we consider a single spin-dependent impurity of strength  $V_d$  at site  $x$  modeled by the Hamiltonian  $H_d = V_d(c_{\uparrow,x}^\dagger c_{\uparrow,x} - c_{\downarrow,x}^\dagger c_{\downarrow,x})$  (see Fig. 4, left panel), and a spin-independent impurity modeled by the Hamiltonian  $H_d = V_d \sum_{\sigma} c_{\sigma,x}^\dagger c_{\sigma,x}$  (see Fig. 4, right panel). The spin-independent impurity does not have a strong influence on the dynamics of the wave packet, even for an impurity strength  $V_d = 1.5/T$ . By contrast, the spin-dependent impurity is found to cause significant scattering, but the scattered wave packet has both reversed direction of motion and reversed spin polarization, thus keeping the spin-momentum locking intact.

*Concluding discussion.*—For periodically driven 2D systems, it has recently been shown [12] how chiral edge states can occur, even if all quasienergy bands are characterized by a zero Chern number—a no go for static systems. In our present Letter, even without any 2D bulk, we have found a 1D Floquet counterpart [see Eq. (1)] of helical edge states known from 2D topological insulators. Since Eq. (1) cannot be realized as a local Hamiltonian in a static microscopic 1D lattice model, our results give a new intriguing example of how periodically driven systems can dynamically enable the realization of exotic states of matter. Remarkably, the microscopic model (2) and driving protocol proposed here is of immediate experimental relevance as it can be implemented by combining state-of-the-art techniques to trap and manipulate ultracold quantum gases.

We note that a unidirectional motion has been recently realized [34,35] in quantum walk setups [36–38] in a photonic context. There, the essential physical mechanism relies on the higher spatial dimension of the setup: A beam displacer redirects the unidirectional motion of the incident laser beam into a step of the walk in a perpendicular direction. By contrast, here we are interested in a fermionic quantum many-body system in a microscopic 1D lattice potential, where the dynamics is constrained by fermion doubling. In an atomic setup, a unidirectional quantum walk has been engineered based on the adiabatic modulation of spin-dependent lattice potentials (see, e.g., [39,40]), while our present driving protocol is based on a stationary lattice potential and does not rely on adiabatic assumptions.

In a broader context, helical channels have been identified as promising candidates for numerous applications. In the field of spintronics, their perfect spin-momentum locking may enable new possibilities to control spin properties by all electric means. Regarding the realization of exotic quasiparticles, hybrid systems involving helical channels coupled to superconductors have repeatedly appeared, both in the context of Majorana bound states [41] and, more recently, in the theoretical prediction of fractional Majorana fermions or parafermions in strongly correlated systems [42–44]. The Floquet counterpart of helical channels reported in our present Letter may be of key interest along these lines: First, from a computational perspective, our microscopic 1D lattice model (2) will even in the presence of pairing terms and correlations still be amenable to first-principles numerical analysis, e.g., by means of time-dependent density matrix renormalization group techniques. Second, the inherently time-dependent character of the proposed system may lead to phenomena in such hybrid systems (see, e.g., Ref. [45] for the example of Floquet Majorana states at finite quasienergy) that are not found in their static counterparts. Finally, the simplicity and feasibility of our proposal hold great promise for the observation of such new physics in future experiments.

This project was supported by the European Research Council (ERC) Synergy Grant UQUAM, and the Spezial-Forschungsbereich (SFB) FoQuS, Austrian Science Fund (FWF) Project No. F4016-N23. Y. H. also acknowledges support from the Institut für Quanteninformaton GMBH.

- 
- [1] V. Galitski and I. B. Spielman, *Nature (London)* **494**, 49 (2013).
- [2] A. Manchon, H. C. Koo, J. Nitta, S. M. Frolov, and R. A. Duine, *Nat. Mater.* **14**, 871 (2015).
- [3] K. Y. Bliokh, F. J. Rodríguez-Fortuño, F. Nori, and A. V. Zayats, *Nat. Photonics* **9**, 796 (2015).
- [4] C. L. Kane and E. J. Mele, *Phys. Rev. Lett.* **95**, 226801 (2005).
- [5] C. Wu, B. A. Bernevig, and S.-C. Zhang, *Phys. Rev. Lett.* **96**, 106401 (2006).
- [6] C. Xu and J. E. Moore, *Phys. Rev. B* **73**, 045322 (2006).
- [7] B. A. Bernevig, T. L. Hughes, and S.-C. Zhang, *Science* **314**, 1757 (2006).
- [8] M. König, S. Wiedmann, C. Brüne, A. Roth, H. Buhmann, L. W. Molenkamp, X.-L. Qi, and S.-C. Zhang, *Science* **318**, 766 (2007).
- [9] M. Z. Hasan and C. L. Kane, *Rev. Mod. Phys.* **82**, 3045 (2010).
- [10] X.-L. Qi and S.-C. Zhang, *Rev. Mod. Phys.* **83**, 1057 (2011).
- [11] H. B. Nielsen and M. Ninomiya, *Phys. Lett.* **105B**, 219 (1981).
- [12] M. S. Rudner, N. H. Lindner, E. Berg, and M. Levin, *Phys. Rev. X* **3**, 031005 (2013).
- [13] N. Goldman and J. Dalibard, *Phys. Rev. X* **4**, 031027 (2014).
- [14] J. Klinovaja, P. Stano, and D. Loss, *Phys. Rev. Lett.* **116**, 176401 (2016).
- [15] P. Titum, E. Berg, M. S. Rudner, G. Refael, and N. H. Lindner, *Phys. Rev. X* **6**, 021013 (2016).
- [16] V. Khemani, A. Lazarides, R. Moessner, and S. L. Sondhi, *Phys. Rev. Lett.* **116**, 250401 (2016).
- [17] A. C. Potter, T. Morimoto, and A. Vishwanath, *Phys. Rev. X* **6**, 041001 (2016).
- [18] C. L. Kane and E. J. Mele, *Phys. Rev. Lett.* **95**, 146802 (2005).
- [19] D. J. Thouless, *Phys. Rev. B* **27**, 6083 (1983).
- [20] M. Lohse, C. Schweizer, O. Zilberberg, M. Aidelsburger, and I. Bloch, *Nat. Phys.* **12**, 350 (2016).
- [21] T. Kitagawa, E. Berg, M. Rudner, and E. Demler, *Phys. Rev. B* **82**, 235114 (2010).
- [22] We note that a complex  $\alpha$  simply amounts to a global shift in the lattice momentum.
- [23] I. Bloch, J. Dalibard, and W. Zwerger, *Rev. Mod. Phys.* **80**, 885 (2008).
- [24] D. Jaksch and P. Zoller, *New J. Phys.* **5**, 56 (2003).
- [25] F. Gerbier and J. Dalibard, *New J. Phys.* **12**, 033007 (2010).
- [26] J. Dalibard, F. Gerbier, G. Juzeliunas, and P. Öhberg, *Rev. Mod. Phys.* **83**, 1523 (2011).
- [27] M. Mancini, G. Pagano, G. Cappellini, L. Livi, M. Rider, J. Catani, C. Sias, P. Zoller, M. Inguscio, M. Dalmonte, and L. Fallani, *Science* **349**, 1510 (2015).
- [28] B. K. Stuhl, H.-I. Lu, L. M. Ayccock, D. Genkina, and I. B. Spielman, *Science* **349**, 1514 (2015).
- [29] J. C. Budich, C. Laflamme, F. Tschirsich, S. Montangero, and P. Zoller, *Phys. Rev. B* **92**, 245121 (2015).
- [30] A. Celi, P. Massignan, J. Ruseckas, N. Goldman, I. B. Spielman, G. Juzeliunas, and M. Lewenstein, *Phys. Rev. Lett.* **112**, 043001 (2014).
- [31] N. Goldman, J. C. Budich, and P. Zoller, *Nat. Phys.* **12**, 639 (2016).
- [32] S. S. Chern, *Ann. Math.* **47**, 85 (1946).
- [33] D. J. Thouless, M. Kohmoto, M. P. Nightingale, and M. den Nijs, *Phys. Rev. Lett.* **49**, 405 (1982).
- [34] M. A. Broome, A. Fedrizzi, B. P. Lanyon, I. Kassal, A. Aspuru-Guzik, and A. G. White, *Phys. Rev. Lett.* **104**, 153602 (2010).
- [35] T. Kitagawa, M. A. Broome, A. Fedrizzi, M. S. Rudner, E. Berg, I. Kassal, A. Aspuru-Guzik, E. Demler, and A. G. White, *Nat. Commun.* **3**, 882 (2012).
- [36] T. Kitagawa, M. S. Rudner, E. Berg, and E. Demler, *Phys. Rev. A* **82**, 033429 (2010).
- [37] B. Tarasinski, J. K. Asboth, and J. P. Dahlhaus, *Phys. Rev. A* **89**, 042327 (2014).
- [38] J. K. Asboth and J. M. Edge, *Phys. Rev. A* **91**, 022324 (2015).
- [39] M. Karski, L. Förster, J. Choi, A. Steffen, W. Alt, D. Meschede, and A. Widera, *Science* **325**, 174 (2009).
- [40] C. S. Hamilton, R. Kruse, L. Sansoni, C. Silberhorn, and I. Jex, *Phys. Rev. Lett.* **113**, 083602 (2014).
- [41] L. Fu and C. L. Kane, *Phys. Rev. Lett.* **100**, 096407 (2008).
- [42] F. Zhang and C. L. Kane, *Phys. Rev. Lett.* **113**, 036401 (2014).
- [43] C. P. Orth, R. P. Tiwari, T. Meng, and T. L. Schmidt, *Phys. Rev. B* **91**, 081406 (2015).
- [44] J. Alicea and P. Fendley, *Annu. Rev. Condens. Matter Phys.* **7**, 119 (2016).
- [45] L. Jiang, T. Kitagawa, J. Alicea, A. R. Akhmerov, D. Pekker, G. Refael, J. I. Cirac, E. Demler, M. D. Lukin, and P. Zoller, *Phys. Rev. Lett.* **106**, 220402 (2011).